SPARSE WAVE-EQUATION DECONVOLUTION IMAGING FOR IMPROVED SHALLOW WATER DEMULTIPLE

G. Poole[1], H. Moore[1], E. Blaszczak[1], H. Kerrison[1], S. Keynejad[1], A. Taboga[1], M. Chappell[1]

[1] CGG

Summary

The attenuation of surface related multiples is typically one of the most challenging steps in the processing of shallow water marine projects. Least-squares wave-equation deconvolution imaging is a powerful tool to address this challenge, but images derived from a deep target level may produce sub-optimal demultiple results for the shallower section. We introduce image domain sparseness weights to the least-squares problem, derived from a water-bottom depth estimate. This provides a reflectivity with a sharp contrast at the water-bottom, and the corresponding multiple prediction exhibits improved temporal resolution compared to least-squares wave-equation deconvolution imaging. We also illustrate how the multiple prediction from sparse wave-equation deconvolution imaging may be combined with source-side targeted multiple prediction to improve multiple attenuation for complex multiple generators. Data examples from the Central North Sea and the West of Shetland confirm the benefits of the proposed methods in attenuating residual multiples.

Sparse wave-equation deconvolution imaging for improved shallow water demultiple

Introduction

Most surface related multiple prediction methods involve convolving data with an estimate of the multiple generators (for example, SRME, Berkhout and Verschuur, 1997). In deep water marine settings the field data itself is generally recorded well enough to use as a representation of the multiple generators. The resulting multiple model is then adaptively subtracted from the recorded data to account for inaccuracies such as source wavelet squaring and cross-talk between multiples. An alternative method, SRMM, using wavefield extrapolation, was described by Pica et al. (2005).

In shallow water settings, the minimum acquired offset is often not small enough to record the multiple generators accurately enough for SRME or SRMM. In this case, targeted multiple prediction methods assuming the depth of the multiple generator are often employed (Wiggins, 1988 or Wang et al., 2011). Gapped deconvolution offers an alternative to targeted approaches, however implementations are typically limited to two dimensions (Biersteker, 2001) due to a lack of shotpoint coverage in 3D as well as high runtimes. Higher order corrections may be applied to compensate for amplitude inconsistencies between consecutive orders of multiple (Backus, 1959 and Lokshtanov, 1993). Poole (2019) described a 3D deconvolution-like approach where the multiple prediction operator was defined in the image domain. The resulting image was used as input to the multiple prediction approach of Pica et al. (2005).

We further develop the approach of Poole (2019) to derive image domain sparseness weights corresponding to the water-bottom reflection and demonstrate that this improves the temporal resolution of modelled water-layer related multiples. In addition, we show how the method may be used in combination with source-side targeted multiple prediction for further improved multiple attenuation.

Methodology

As described by Equation 1, Poole (2019) derived a reflectivity, $r(x,y,z)$, which, when convolved with the forward extrapolated down-going wavefield, $D_\Phi(f,x,y,z)$, and subsequently extrapolated forward to the surface using an operator $\Phi(f,x,y,z)$, resulted in estimated multiples, $m(t,x,y)$, subject to data domain confidence weights, $C(t,x,y)$. Here, (x,y,z) refer to spatial coordinates, t and f refer to time and temporal frequency respectively, and transformations from the frequency domain to the time domain are obtained using the temporal inverse Fourier transform, F^{-1}. The recorded data was substituted as a proxy for the multiples, m, and a minimum image depth constrained the approach to reduce degrees of freedom, analogous to the use of a deconvolution gap.

$$m(t,x,y) = C(t,x,y)F^{-1}\Phi(f,x,y,z)D_\Phi(f,x,y,z)r(x,y,z) \tag{1}$$

Various extrapolation operators may be used, for example phase shift plus interpolation, finite difference, or Fourier finite difference (see Biondi, 2006, for more information). The method is similar to multiple prediction using gapped deconvolution, but uses the reflectivity to represent the prediction operator. As with gapped deconvolution, the design window should be at the depth level of geological interest. For deep design windows, attenuation may have absorbed the higher frequencies and the resulting reflectivity may be dominated by low frequencies. The corresponding multiple model will also be lacking in higher frequencies, limiting demultiple effectiveness in the shallow section. While we may derive the reflectivity in the shallow section, this may not be optimal for multiple attenuation at target.

Following Trad et al. (2003) we add image domain sparseness weights, $S(x,y,z)$, to Equation 1, as given by Equation 2. $S(x,y,z)$ is a diagonal matrix operator, scaling each value of $\hat{r}(x,y,z)$.

$$m(t,x,y) = C(t,x,y)F^{-1}\Phi(f,x,y,z)D_\Phi(f,x,y,z)S(x,y,z)\hat{r}(x,y,z) \tag{2}$$

We define the sparseness weights to be zero above the water-bottom, a fixed-amplitude spike at the water-bottom, and a lower-amplitude constant below the water-bottom, based on the following:

1) Least-squares inversion to find r in Equation 1.
2) Pick the water-bottom arrival.
3) Define sparseness; spike at the water-bottom followed by a lower amplitude constant.

The fixed-amplitude spike ensures a sharp water-bottom reflectivity, resulting in a full-bandwidth water-layer multiple prediction. The ratio of the spike to the constant defines the importance of the water-bottom as a multiple generator inside the inversion. In practice we have found using ratios in the range 2 to 6 produce good results. After deriving the sparseness, we solve Equation 2 for $\hat{r}(x, y, z)$, then multiply by S to obtain the final reflectivity used for multiple prediction based on Pica et al. (2005).

While the approach may be modified to predict both source- and receiver-side multiples, in practice towed streamer data is not sampled well enough on the source side for this to be effective. As a result, we propose to combine source-side targeted multiple prediction (Wang et al., 2011) with sparse wave-equation deconvolution prediction on the receiver-side.

Data examples

The first data example comes from a 35,000 sq-km mega-survey located in the Central North Sea, combining 31 separate towed streamer surveys acquired over a 20 year period. The shallow water nature of the area resulted in prevalent free surface multiples creating a curtain of interference following each primary reflection, Figure 4a. Figure 1a shows reflectivity resulting from the least-squares imaging. The water-bottom reflection as well as shallow channels and dipping layers can be observed. The sparseness derived from this initial reflectivity is shown in Figure 1b, and the corresponding sparse inversion reflectivity is given in Figure 1c. The sparse reflectivity exhibits a sharp reflector at the water-bottom, but still has the same deeper geological content as the least-squares reflectivity. Figure 2 shows a depth slice from the reflectivity volume at 115 m, highlighting the lateral complexity of the multiple generators below the water-bottom. While a slight acquisition pattern may be noticed, due to different surveys being acquired in different directions, the reflectivity is generally spatially consistent across the area.

Figure 1 *a) Least-squares reflectivity, b) sparseness weights with inset filled wiggle trace, and c) sparse inversion reflectivity using weights from b).*

Figure 2 *Depth slice from the reflectivity at 115 m.*

Figure 3 shows an input shot gather (a) along with multiple predictions corresponding to reflectivity models derived using least-squares (b) and sparse inversion (c). The sparse inversion result exhibits a more detailed multiple prediction with higher temporal resolution.

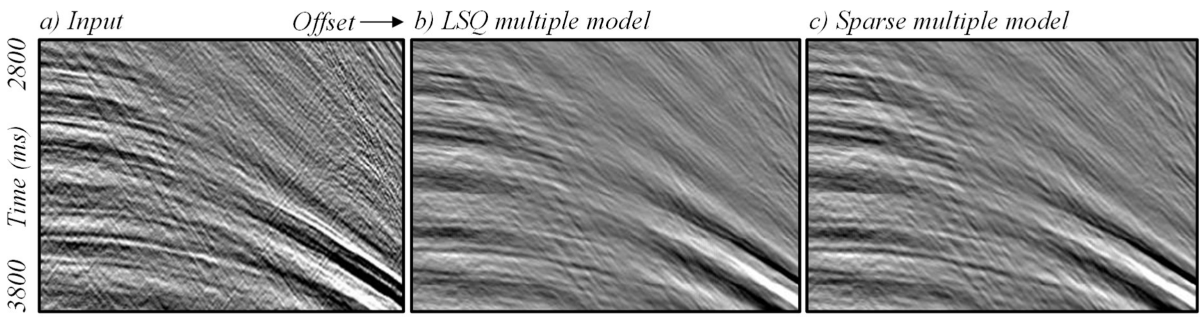

Figure 3 *Shot gather display: a) data before demultiple, b) multiple prediction from the least-squares image, and c) multiple prediction from the image derived using sparse inversion.*

Figure 4 shows a migrated stack corresponding to data before demultiple (a) along with demultiple results using reflectivity derived by least-squares inversion (b) and sparse inversion (c). The arrows highlight areas where the multiple attenuation is more effective with the sparse inversion approach.

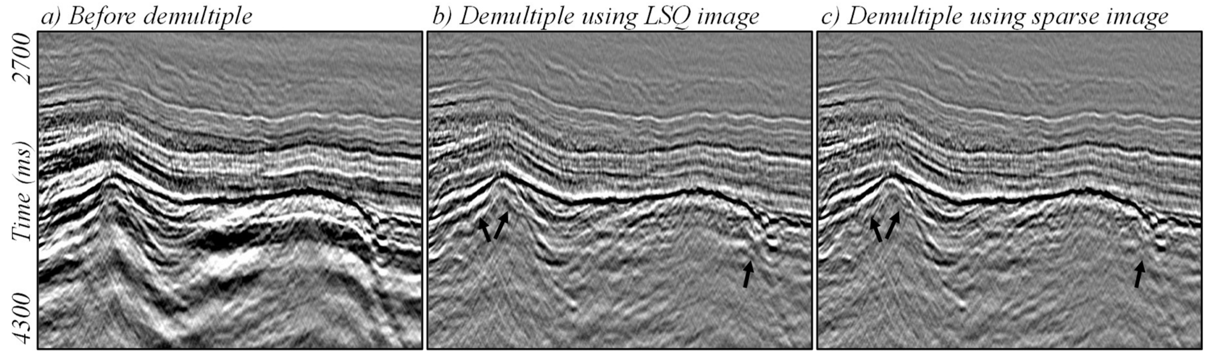

Figure 4 *Migrated stack comparison for data: a) before demultiple, b) after demultiple using the image from least-squares inversion, and c) after demultiple using the image from sparse inversion.*

The second data example comes from an acquisition West of Shetland in the North Atlantic (Poole et al., 2019). The water depth in this area varies from 100 m to 650 m. Figure 5 shows a depth image of the shallow section relating to primary imaging (a), least-squares deconvolution imaging (b), and sparse deconvolution imaging (c). The primary image exhibits high levels of stretch and a lack of spatial resolution due a lack of primary reflections, making it unsuitable for multiple prediction. The least-squares deconvolution image exhibits improved spatial resolution, the sparse deconvolution image additionally has a sharper water-bottom reflection.

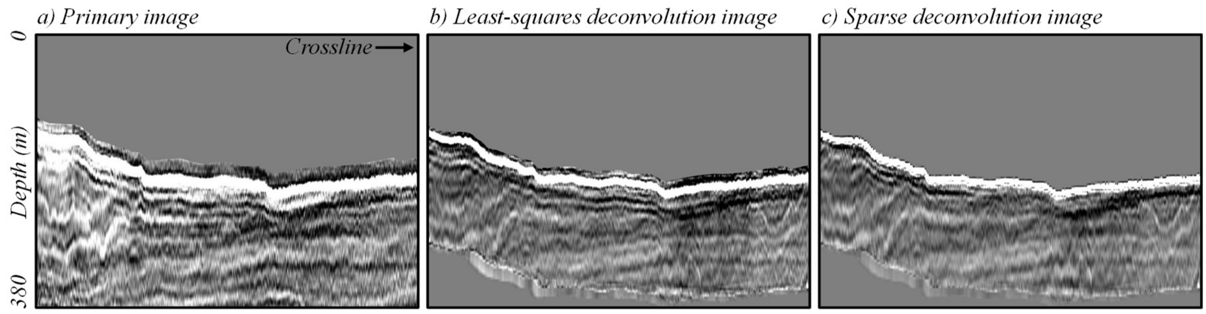

Figure 5 *Shallow imaging results corresponding to: a) primary image, b) least-squares deconvolution image, and c) sparse deconvolution image.*

As well as the complications of a shallow water depth, this area also exhibited issues relating to 3D volcanic sills in the shallow section as shown in the migrated data before demultiple in Figure 6a. These multiple generators created a complex set of diffracted arrivals as shown on the depth slice (Figure 6b). As described earlier, the sparse deconvolution imaging method predicts receiver-side multiples only. While in less geologically complex areas receiver-side multiples may be kinematically similar to source-side multiples, in this example a clear difference may be observed from receiver-side (d) and source-side (e) targeted multiple predictions (MWD; Wang et al., 2011). For example, the diffracted source-side multiples on the left hand side (black arrows) are more pronounced than on the right, whereas the opposite is the case for the receiver-side multiples (white arrows). The sparse deconvolution multiple model closely resembles the kinematics of the receiver-side MWD model, as expected.

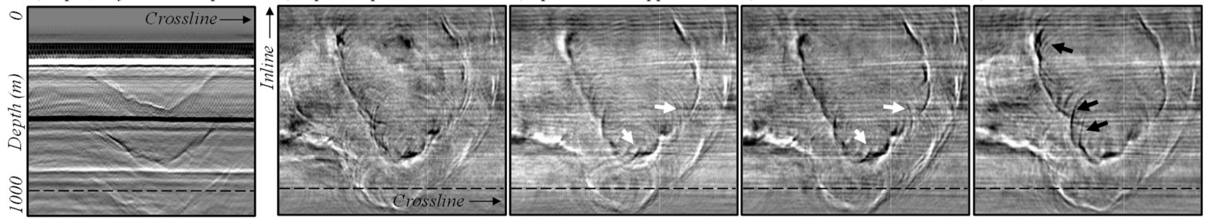

Figure 6 *Migrated stack comparison of: Inline: a) data before demultiple; depth slice at 900 m: b) data before demultiple, c) multiple model from sparse wave-equation deconvolution, d) receiver-side MWD, and e) source-side MWD.*

Figure 7 shows a stack section of data before demultiple (a), after demultiple using 3D recursive MWD following Cooper et al. (2015) (b), and after demultiple using joint sparse wave-equation deconvolution and source-side MWD (c). A reduction in the level of residual multiple may be seen on the joint approach as highlighted by the arrows.

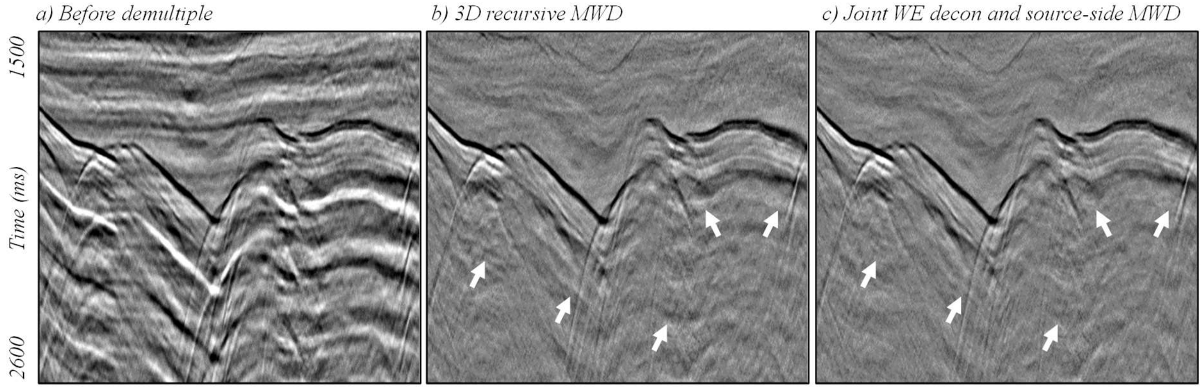

***Figure** 7 Stack displays for: a) input to demultiple, b) demultiple using 3D recursive MWD, and c) demultiple combining sparse wave-equation deconvolution with source-side MWD.*

Conclusions

We have introduced a method to derive image domain sparseness weights to input to a sparse wave-equation deconvolution imaging approach. The approach results in an image with a highly focussed water-bottom, providing a subsequent multiple prediction step with improved temporal resolution. We have also illustrated the limitations of receiver-side multiple predictions, and how these limitations may be alleviated by combining with source-side multiple models from targeted multiple prediction methods. Shallow water data examples from the Central North Sea and West of Shetland have shown how these approaches offer an improvement in the attenuation of residual multiples.

Acknowledgements

The authors would like to thank CGG Multi-Client & New Ventures for permission to show the data examples and CGG for allowing us to publish this work.

References

Backus, M.M. [1959] Water reverberations – their nature and elimination. *Geophysics*, **24**, 233-261.

Berkhout, A.J. and Verschuur, D.J. [1997] Estimation of multiple scattering by iterative inversion, Part I: theoretical considerations. *Geophysics*, **62**, 1586-1595.

Biersteker, J. [2001] MAGIC: Shell's surface multiple attenuation technique. *71st Annual International Meeting,* SEG, Expanded Abstracts, 1301-1304.

Biondi, B.L. [2006] 3D seismic imaging. *Investigations in Geophysics*, Society of Exploration Geophysicists publication.

Cooper, J., Poole, G., Wombell, R. and Wang, P. [2015] Recursive model-based water-layer demultiple. *77th EAGE Conference and Exhibition*, Extended Abstracts, Tu N114 2.

Lokshtanov, D.E. [1993] Adaptive multiple suppression in tau-p domain. *63nd Annual International Meeting,* SEG, Expanded Abstracts, 1086-1089.

Pica, A., Poulain, G., David, B., Magesan, M., Baldock, S., Weisser, T., Hugonnet, P. and Herrmann, P. [2005] 3D surface-related multiple modeling, principles and results. *75th Annual International Meeting*, SEG, Expanded Abstracts, 2080-2083.

Poole, G. [2019] Shallow water surface related multiple attenuation using multi-sailline 3D deconvolution imaging. *81st EAGE Conference and Exhibition*, Extended Abstracts, Tu R1 5.

Poole, G., Page, C., James, G., Wombell, R., Mensch, T., Flower, R., Kaszycka, E., Cichy, K., Davies, D., Saxton, L. and Harrison, D. [2019] Rich azimuth dual triple-source simultaneous shooting West of Shetland. *81st EAGE conference & exhibition*, Extended abstracts, Tu R9 13.

Wang, P., Jin, H., Xu, S. and Zhang, Y. [2011] Model-based water-layer demultiple. *81st Annual International Meeting,* SEG, Expanded Abstracts, 3551-3555.

Wiggins, W. [1988] Attenuation of complex water-bottom multiples by wave-equation-based prediction and subtraction. *Geophysics*, **53**, 1527-1539.